

# Gas migration process in deformable clay formations

**Enrique Romero<sup>1</sup>, Laura Gonzalez-Blanco<sup>1</sup>**

<sup>1</sup>Universitat Politècnica de Catalunya, Barcelona, Spain. [enrique.romero-morales@upc.edu](mailto:enrique.romero-morales@upc.edu)

## Introduction

To predict the evolution of a Geological Disposal Facility, it is necessary to understand the interaction between a number of key features and process and its impact on the long-term behaviour. Central to these issues are the mechanisms and process that govern the movement of gases in a repository. Linking the gas transport to the stress-strain response of the engineering systems barriers remains challenging particularly from an experimental point of view. Therefore, this paper aims to shed light on the volume change response of different potential host clayey rocks -Boom Clay formation from Belgium and Opalinus Clay and 'Brauner Dogger' formations from Switzerland- during gas injection and dissipation experiments through a comparative study.

## Materials used in the research

Boom Clay (BC) cores were recovered at a depth of 223 m from the URL at Mol, Belgium. Four different core samples were retrieved from a deep geothermal well near Schlattigen in the Molasse Basin of North-eastern Switzerland, two of them were recovered from a clay-rich sequence at depths 777 and 782 m bg, called 'Brauner Dogger' (BD) (strata of the Upper Dogger) and the two remaining cores were taken from the Opalinus Clay formation (OPA) at depths 880 and 936 m bg. Initial conditions of the samples are summarised in Table 1. Mercury intrusion porosimetry MIP tests revealed mono-modal pore size density functions with decreasing dominant entrance pore sizes and increasing air-entry values at increasing depths, as indicated in the table. Samples displayed high initial suctions (between 2.5 and 44 MPa), despite being nearly saturated, due to stress relief disturbances.

Table 1. Initial conditions of the samples

Formation	Boom Clay		'Brauner Dogger'		Opalinus Clay	
	BC (223 m)	OED 20/Harz (776 m)	EMPA SLA (781 m)	OED (880 m)	OED 1/1 (936 m)	
Core-sample reference	BC (223 m)	OED 20/Harz (776 m)	EMPA SLA (781 m)	OED (880 m)	OED 1/1 (936 m)	
Density of solids $\rho_s$ (Mg/m <sup>3</sup> )	2.67	2.69	2.69	2.69	2.69	2.69
Plastic limit $w_p$ (%)	29	18	17	--	18	18
Liquid limit $w_L$ (%)	67	28	24	--	29	29
Dominant entrance pore mode from MIP (nm)	65	20	22	16	< 8	< 8
Air-entry value from dominant entrance pore size (MPa)	4.8	14	13	18	> 37	> 37
Dry density $\rho_d$ (Mg/m <sup>3</sup> )	1.66-1.69	2.38 - 2.41	2.48	2.42 - 2.43	2.43	2.43
Void ratio $e$	0.58-0.61	0.116 - 0.130	0.09	0.107 - 0.112	0.11	0.11
Water content $w$ (%)	22.6-24.0	4.34 - 5.43	4.78	4.30 - 4.70	4.79	4.79
Degree of saturation $S_r$	around 1.0	around 1.0	0.95 - 1.0	1.0	0.98 - 1.0	0.98 - 1.0
Total suction $\Psi$ (MPa)	2.45	5	37	4	44	44

## Experimental equipment

On one hand, a high-pressure oedometer cell was used to determine the compressibility parameters of all samples and to carry out the air injection experiments on Boom Clay samples at two different orientations (bedding planes orthogonal and parallel to axis/flow). On the other hand, injection experiments of OPA and BD samples were performed on a high-pressure isotropic cell.

The tests protocols for the injection tests were very similar for all the samples. Controlled-volume rate air injection experiments (0.04, 2 and 100 mL/min), followed by shut-in and dissipation stages were performed under constant vertical or isotropic stress conditions (total vertical stress  $\sigma_v=6$  MPa or total mean stresses  $p=15$  MPa and 19 MPa). The protocol included: a) pre-conditioning (loading to in situ stress state at constant water content); b) soaking with artificial pore water and measurement of water permeability; c) vertical or isotropic drained loading; and d) controlled-rate air injection at upstream/bottom cap, followed by shut-in and recovery phases at constant  $\sigma_v$  or  $p$ .

## Experimental results and interpretation

Air injection experiments in these formations show a common behaviour. The air pressurization process acts as an unloading stage at constant vertical or isotropic stress, inducing the expansion of the samples and causing some degradation in terms of opening of fissures. Regarding the fast air injection tests, the expansion of the samples presented some delay while the air pressure front propagated. In contrast, at slower rates, almost all the expansion occurred during the injection, since the pore pressures inside the samples were nearly equilibrated. Maximum expansions on pore pressure increase were observed on Opalinus Clay compared to 'Brauner Dogger', consistent with compressibility results on loading/unloading. The expansion was larger on Boom Clay samples tested with bedding planes orthogonal to flow. Some elapsed time after shut-in, samples underwent some compression along the dissipation stage due to the air pressure decrease and thus, constitutive stress increase.

In order to characterize how the porosity network was modified by the air injection process, MIP tests were carried out before (intact state) and after air tests. A new family of large pores, which was not detected on intact samples, was systematically observed after each injection test. This new dominant pore size at entrance sizes larger than 2  $\mu\text{m}$  was associated with the expansion (and degradation) undergone by the material during the air injection stage when the constitutive stress decreased (Figure 1). A fractal analysis of the data showed that the macroporosity tended to a fissure-like shape.

Intrinsic permeability to air was affected by fissure opening since preferential paths were generated, enhancing the air flow. An exponential increase of the air permeability with the proportion of fissures detected by MIP technique ( $e_{\text{fissure}}/e_{\text{total}}$ ) was experimentally observed for Boom Clay samples (Figure 2).

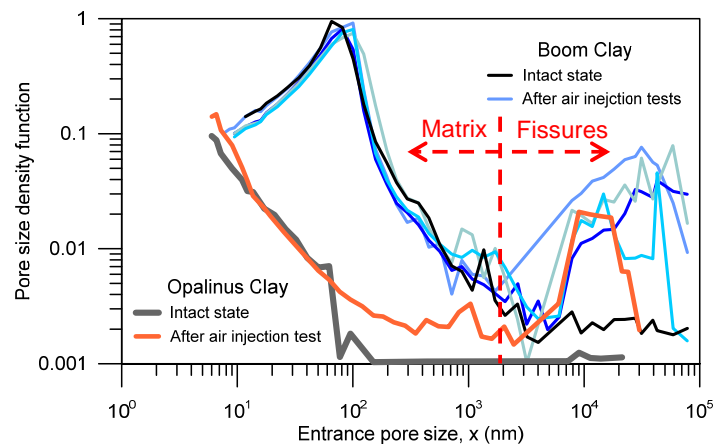


Figure 1. Changes in pore size distribution before and after air injection tests for Opalinus Clay and Boom Clay samples.

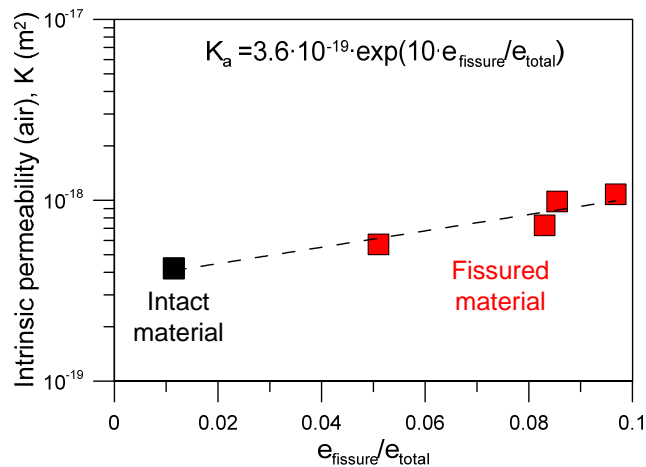


Figure 2. Exponential fitting of intrinsic permeability values in terms of the proportion of fissures on Boom Clay samples.